

(7) NOTICE. THIS MATERIAL MAY BE PROTECTED
BY COPYRIGHT LAW (TITLE 17 U.S. CODE)

Inactivation of TNF Signaling by Rationally Designed Dominant-Negative TNF Variants

Paul M. Steed,^o Malú G. Tansey,^{o,†} Jonathan Zalevsky,^o
Eugene A. Zhukovsky, John R. Desjarlais, David E. Szymkowski,
Christina Abbott, David Carmichael, Choryl Chan, Lisa Chorri,
Peter Cheung, Arthur J. Chirino, Hyo H. Chung, Stephan K. Doberstein,
Araz Elvazi, Anton V. Filikov, Sarah X. Gao, René S. Hubert,
Mariam Hwang, Linus Hyun, Sandhya Kashi, Alice Kim, Esther Kim,
James Kung, Sabrina P. Martinez,[†] Umesh S. Muchhal,
Duc-Hanh T. Nguyen, Christopher O'Brion, Donald O'Keeffe,
Karen Singer, Omid Vafa, Jost Vielmetter, Sean C. Yoder,
Bassil I. Dahiyat,[†]

Copyright Clearance Center for the American
Chemical Society and the American Association
of Immunologists, Inc.

BEST AVAILABLE COPY

estimated between 20,000 and 40,000 metric tons (10, 12). Assuming that pre-Incan technologies operated at efficiencies comparable to *huayras* and recognizing the initial presence of grades as rich as 25% Ag (11), our data imply that several thousand tons of silver were produced in pre-Incan times. Although major new archaeological discoveries in the Andes remain a distinct possibility, the likelihood seems equally probable that most of this silver was recycled and transported elsewhere in the Americas before conquest, or eventually exported overseas by the Spanish.

References and Notes

1. H. Lechtman, in *The Coming of the Age of Iron*, P. J. Vertime, J. D. Muhly, Eds. (Yale Univ., New Haven, CT, 1980), pp. 267–334.
2. R. L. Burger, R. B. Gordon, *Science* **282**, 1108 (1998).
3. E. P. Benson, Ed., *Pre-Columbian Metallurgy of South America* (Dumbarton Oaks, Washington, DC, 1979).
4. I. Shennan, S. Epstein, A. K. Craig, *Science* **216**, 952 (1982).
5. H. Lechtman, in *Tiwanaku and Its Hinterland: Archaeology and Paleoenvironment of an Andean Civilization* Vol. 2, A. L. Kolata, Ed. (Smithsonian Institution, Washington, DC, 2002), pp. 404–434.
6. K. O. Bruhns, *Ancient South America* (Cambridge Univ., Cambridge, 1994).
7. W. E. Rudolph, *Am. Geogr. Soc.* **26**, 529 (1936).
8. M. Vuille, *Int. J. Climatol.* **19**, 1579 (1999).
9. Materials and methods are available as supporting material on Science Online.
10. P. J. Bartos, *Econ. Geol.* **95**, 645 (2000).
11. W. E. Wilson, A. Petrov, *Miner. Rec.* **30**, 9 (1999).
12. P. J. Bakewell, *Miners of the Red Mountain: Indian Labor in Potosí 1545–1650* (Univ. of New Mexico, Albuquerque, NM, 1984).
13. R. Peele, *Sch. Mines Q.* **15**, 8 (1893).
14. L. Renberg, I. M. Wik-Persson, O. Emteryd, *Nature* **368**, 323 (1994).
15. M. L. Brämhöv, R. Bindler, O. Emteryd, L. Renberg, *J. Paleolimnol.* **25**, 421 (2001).
16. C. Cobell, *Environ. Sci. Technol.* **33**, 2953 (1999).
17. L. Rivera-Duarte, A. R. Flegal, *Geochim. Cosmochim. Acta* **58**, 3307 (1994).
18. B. B. Wolfe, *Palaeogeogr. Palaeoclim. Palaeoecol.* **176**, 177 (2001).
19. A. S. Et, L. Renberg, *J. Paleolimnol.* **26**, 89 (2001).
20. A. F. Bandelier, *The Islands of Thicoco and Kosti* (Hispanic Society of America, New York, 1910).
21. P. R. Williams, *World Archaeol.* **33**, 361 (2002).
22. A. L. Kolata, *The Tiwanaku: Portrait of an Andean Civilization* (Blackwell, Oxford, UK, 1993).
23. M. B. Abbott, M. W. Binford, M. Brenner, K. R. Keats, *Quat. Res.* **47**, 169 (1997).
24. B. S. Bauer, C. Sharpen, *Ritual and Pilgrimage in the Ancient Andes: The Islands of the Sun and the Moon* (Univ. of Texas, Austin, TX, 2001).
25. L. G. Thompson, E. Mosley-Thompson, J. F. Bolzan, B. R. Koci, *Science* **229**, 971 (1985).
26. A. K. Craig, in *Precious Metals, Cobre, and the Changes in Monetary Structures in Latin America, Europe, and Asia*, E. van Cauwenbergh, Ed. (Leuven Univ. Press, Leuven, Netherlands, 1989), pp. 159–183.
27. G. E. Erickson, R. G. Luedke, R. L. Smith, R. P. Koeppen, F. Urquidi, *Episodes* **13**, 5 (1990).
28. Supported by the U.S. NSF-ESH (M.B.A.), Natural Sciences and Engineering Research Council of Canada (A.P.W.) and Geological Society of America. We are grateful to H. Lechtman, M. Bernmark, C. Cooke, and journal reviewers for their insightful comments; G. Seltzer for assistance in the field; and S. Root for support in the laboratory.

Supporting Online Material
www.sciencemag.org/cgi/content/full/301/5641/1893/DC1

Materials and Methods
Fig. S1
Tables S1 and S2

9 June 2003; accepted 18 August 2003

Tumor necrosis factor (TNF) is a key regulator of inflammatory responses and has been implicated in many pathological conditions. We used structure-based design to engineer variant TNF proteins that rapidly form heterotrimers with native TNF to give complexes that neither bind to nor stimulate signaling through TNF receptors. Thus, TNF is inactivated by sequestration. Dominant-negative TNFs represent a possible approach to anti-inflammatory biotherapeutics, and experiments in animal models show that the strategy can attenuate TNF-mediated pathology. Similar rational design could be used to engineer inhibitors of additional TNF superfamily cytokines as well as other multimeric ligands.

TNF is a proinflammatory cytokine that can complex two TNF receptors, TNFR1 (p55) and TNFR2 (p75), to activate signaling cascades controlling apoptosis, inflammation, cell proliferation, and the immune response (1–5). The 26-kD type II transmembrane TNF precursor protein, expressed on many cell types, is proteolytically converted into a soluble 52-kD homotrimer (6). An elevated serum level of TNF is associated with the pathophysiology of rheumatoid arthritis (RA), inflammatory bowel disease, and ankylosing spondylitis (1, 7, 8), and molecules that inhibit TNF signaling have demonstrated clinical efficacy in treating some of these diseases (9, 10).

We have engineered dominant-negative TNF (DN-TNF) variants that inactivate the native homotrimer by a sequestration mechanism that blocks TNF bioactivity (fig. S1). Protein design automation (PDA), an *in silico* method that predicts protein variants with improved biological properties (11–13), was used to introduce single or double amino acid changes into TNF (Fig. 1A) to generate the desired biological profile while maintaining the overall structural integrity of the molecule. Specifically, our goal was to design

Xencor, 111 West Lemon Avenue, Monrovia, CA 91016, USA.

^oThese authors contributed equally to this work.

[†]Present address: Department of Physiology, University of Texas Southwestern Medical Center at Dallas, Dallas, TX 75390, USA.

[‡]To whom correspondence should be addressed. E-mail: bat@xencor.com

cell-
FR2
NP
anti-
city
3ya-
ism
of
num
by
Fig
t of
and

A145R/I97T attenuated TNF-induced caspase activity by 50%, and at 20-fold excess, activity was reduced to baseline. The *in vitro* potency (by mass) of these variants is comparable to that of a soluble Fc-TNFR2 fusion (etanercept) and more potent than that of an antibody to TNF (infliximab), two marketed anti-TNF therapies, supporting the potential utility of this mechanism. Similarly, at 20-fold excess over native TNF, single-point (A145R, I97T, Y87H) and particularly double-point (A145R/Y87H, A145R/I97T) variants decreased caspase activation (Fig. S3) as well as TNF-induced transcriptional activation by NF- κ B in human embryonic kidney (HEK)

293T cells (Fig. 2B). Consistent with these results, the TNF variant A145R/Y87H (at 10-fold excess over native TNF) blocked TNF-induced nuclear translocation of the NF- κ B p65-RelA subunit in HeLa cells (Fig. 2C). Thus, a number of variants neutralized TNF-induced caspase and NF- κ B-mediated transcriptional activity over a wide range of native TNF concentrations, including the clinically relevant range of 100 to 200 pg/ml found in the synovial fluid of RA patients (17–19).

To demonstrate that the mechanism of TNF inhibition requires the formation of heterotrimeric complexes with native TNF, we measured

the relation between heterotrimer levels and inhibition of TNF-induced signaling (14). We generated heterotrimeric complexes by mixing a fixed amount of FLAG-tagged native TNF with increasing concentrations of His-tagged TNF variants. A part of this material was used in a sandwich enzyme-linked immunosorbent assay (ELISA) (Fig. 3A, open symbols) to detect the formation of His-FLAG heterotrimers, and the remainder was applied to U937 cells to detect TNF-mediated caspase activation (Fig. 3A, closed symbols). The extent of heterotrimer formation of A145R/Y87H or A145R/I97T with native TNF correlated with a decrease in caspase activation, demonstrating an inverse relation between signaling and heterotrimer formation. As expected, etanercept activity is independent of TNF monomer exchange (Fig. 3A, open circles) because etanercept binds to the TNF trimer. To directly visualize heterotrimer formation, we mixed FLAG-tagged native TNF with His-tagged DN-TNF and resolved the exchanged products using native polyacrylamide gel electrophoresis (PAGE) (Fig. 3B) (20). Electrophoresis of equimolar quantities of mixed DN-TNF and native TNF resolved the variant homotrimer, 1:2 and 2:1 native:variant heterotrimers, and native homotrimer in approximately the expected 1:3:3:1 ratio (Fig. 3B, lane 10:10). Western blot analyses (14) with antibodies against the epitope tags confirmed the composition of the intermediate species (Fig. S4). Stochastic equilibrium modeling of native and variant TNF heterotrimer assembly predicts that 10-fold excess of variant homotrimer causes the loss of more than 99% of homotrimeric native TNF, primarily into 1:2 native:variant heterotrimers, and our results confirmed this (Fig. 3B, lane 10:100). Exchange reactions between native and variant TNF reached ~80% completion at 20 min, and essentially all the native homotrimer was depleted after 90 min (Fig. S5). Finally, we confirmed that biological activity of variants requires exchange into heterotrimeric complexes with native TNF. Specifically, our most potent variants (e.g., A145R/Y87H) failed to block caspase activity induced by chemically cross-linked native TNF homotrimers (14), which are unable to dissociate to allow exchange with variant TNFs (Fig. S6).

The most potent *in vitro* inhibitors were selected for testing *in vivo*, to further study the mechanism and to begin therapeutic lead candidate identification. We tested the bioactivity of variant homotrimer and native:variant heterotrimers in the D-galactosamine (GalN)-sensitized mouse model, which demonstrated that DN-TNF homotrimers, and heterotrimers with native TNF, are devoid of agonist activity and efficiently exchange with endogenous TNF *in vivo*. GalN is a known specific hepatotoxic that can increase the sensitivity of mice to human TNF by 1000-fold (21, 22). Native human TNF (30 μ g/kg) induced severe hepatocellular apoptosis and lethality, consistent with previous reports

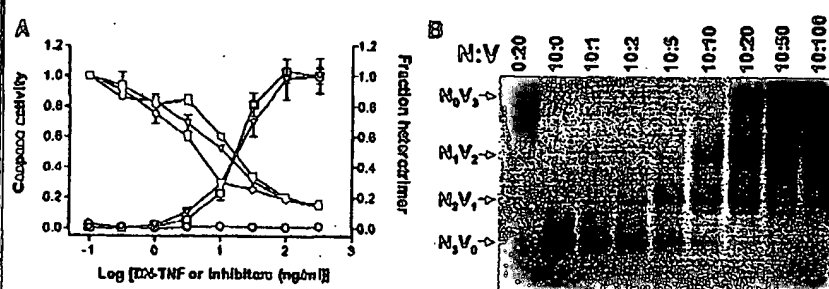


Fig. 3. DN-TNF variants inhibit signaling by sequestering native TNF into inactive heterotrimers. (A) Inverse correlation between heterotrimer formation and caspase activity. Native TNF was mixed in exchange buffer (14) with A145R/Y87H (filled circles), A145R/I97T (open squares), or etanercept (open circles), as described for Fig. 2. A part of each mixture was analyzed by a sandwich ELISA to detect native:variant TNF (open symbols), and the remainder was used to stimulate caspase activity in U937 cells (closed symbols). Caspase activity, arbitrary units normalized to V_{max} . (B) Native gel analysis of heterotrimer formation with various ratios of native (N) and DN-TNF (V). FLAG-tagged native TNF was incubated alone (N_3V_0 , lane 10:0) or with increasing concentrations of His-tagged variant A145R/Y87H (lanes 10:1 to 10:100) before native gel electrophoresis to determine heterotrimer formation. The differences in isoelectric point conferred by the epitope tags allowed for resolution of all possible trimer species (N_3V_0 , N_2V_1 , N_1V_2 , and N_0V_3). Increasing concentrations of DN-TNF variant caused the redistribution of native TNF into both heterotrimers, and at 10-fold excess all detectable native TNF was consumed.

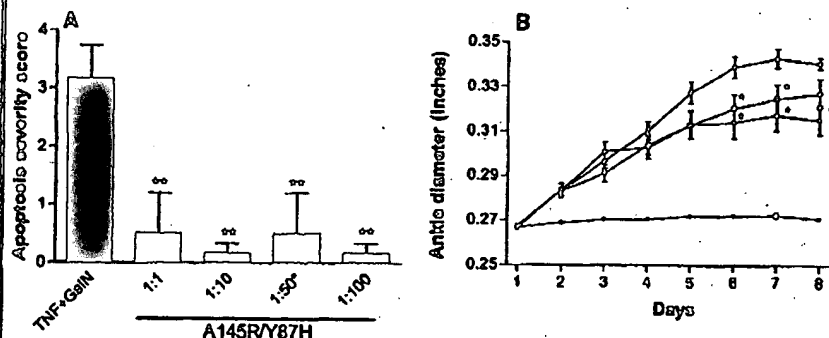


Fig. 4. DN-TNF variants exhibit efficacy in vivo. (A) Effect of heterotrimers of various ratios in the galactosamine-sensitized mouse model of human TNF-induced endotoxicemia. Native human TNF was dosed at 30 μ g/kg and A145R/Y87H was dosed at the indicated ratios to a fixed native human TNF dose of 30 μ g/kg except at the 1:50 ratio, where A145R/Y87H was dosed in 50-fold excess of native human TNF (75 μ g/kg). Livers were harvested and samples were blinded and scored for apoptotic damage on a scale of 0 to 4 as described (14). **P < 0.05. (B) Efficacy of A145R/Y87H in the rat 7-day established CIA model. A145R/Y87H was modified to introduce a PEG moiety at residue 31 of a non-epitope-tagged molecule as described (14). One group of four animals was nonarthritic (open circles); the remaining animals were collagen treated and, after the onset of symptoms, they were randomized into groups of eight. Animals were treated with vehicle (open circles), variant at 10 mg/kg twice daily dosing (filled circles), variant at 2 mg/kg subcutaneously with an intravenous loading dose of 2 mg/kg on the first treatment day (open squares), or variant at 2 mg/kg subcutaneously with an intravenous loading dose of 2 mg/kg on the first treatment day (filled squares). Measurements of ankle diameter were made daily by caliper. *P < 0.05.